

Correlation between Cu^+ -ion instability and persistent spectral hole-burning phenomena of CuCl nanocrystals

Shinji Okamoto* and Yasuaki Masumoto

Institute of Physics and Center for TARA (Tsukuba Advanced Research Alliance), University of Tsukuba, Tsukuba, Ibaraki 305, Japan

(Received 10 February 1997; revised manuscript received 11 August 1997)

We have studied persistent spectral hole-burning (PSHB) phenomena of CuCl nanocrystals embedded in a NaCl crystal. We found correlations between the PSHB phenomena and the photoluminescence spectral changes of excitons in CuCl nanocrystals and of Cu^+ dimers in a NaCl crystal. The spectral changes can be triggered by photoinduced Cu^+ -ion displacements in CuCl nanocrystals and in a NaCl crystal. [S0163-1829(97)03048-8]

Semiconductor nanocrystals have attracted considerable attention not only because of their unique properties but also because of applicability to nonlinear optical devices.^{1,2} For the investigation of the size-dependent properties of nanocrystals, it is ideal to fabricate a well-defined single-sized nanocrystal. However, nanocrystal size is difficult to control in many preparation methods, so that the samples have size distribution and then the absorption bands are inhomogeneously broadened.

Hole-burning spectroscopy is a powerful tool to extract individual and intrinsic information, i.e., information of certain-sized nanocrystals, from the inhomogeneously broadened absorption band. The hole-burning phenomena in the nanocrystal systems were considered to be caused by the absorption saturation of photoexcited carriers, so that the hole spectra had been expected to disappear within a few nanoseconds.

Recently, there have been many reports on persistent spectral hole-burning (PSHB), long-lived hole-burning, or photoinduced absorption-spectral change phenomena of various semiconductor nanocrystals.³ The spectral holes persist for more than a few microseconds or even several hours. Understanding of the mechanism of the PSHB phenomena is indispensable for the understanding of nanocrystals but still poor: The PSHB phenomena were considered to be caused by carrier trapping or photochemical reactions. However, further study is necessary for the understanding of the mechanism.

Ab initio calculations predict that structural instabilities occur in zinc-blende cuprous halides, CuCl, CuBr, and CuI and cause Cu^+ -ion related defects at low temperatures.^{4,5} Such instabilities are expected to induce anomalous phenomena by light irradiation, e.g., persistent photoconductivity in Si-doped GaAs (“DX centers”).⁶ However, there is no experimentally strong evidence of the instabilities in CuCl, and whether the instabilities occur or not is now under discussion.⁷

In this paper, we have investigated a typical sample that exhibits the PSHB phenomena, CuCl nanocrystals embedded in a NaCl crystal, by using the laser-induced spectral-change and temperature-cycle experiments. The experimental results show that the PSHB phenomena can be explained by the two-level-system (TLS) model, in a way analogous to dye

molecule-glass systems. The results also indicate that there are two types of TLS's in the samples. We also found correlations between the PSHB phenomena and photoluminescence (PL) spectral-changes of excitons in CuCl nanocrystals and Cu^+ dimers in NaCl crystals: The absorption and PL spectra are simultaneously modified with an increase of the laser irradiation, and recover at the same cycling temperatures. The spectral-changes can be triggered by Cu^+ -ion displacement in CuCl nanocrystals and NaCl crystals. The *ab initio* calculations of the potential barrier heights for the Cu^+ -ion displacements support this interpretation.

Samples investigated here were CuCl nanocrystals embedded in NaCl crystals. The samples were prepared in the same fashion as is described in Ref. 8. The mean radii of the nanocrystals were determined by small-angle x-ray scattering (SAXS) experiments. The samples were immersed in superfluid helium or mounted on the cold finger of a temperature-variable cryostat. A *Q*-switched Nd^{3+} :YAG (yttrium aluminum garnet) laser, a narrow-linewidth dye laser, and a halogen lamp were used in the experiments. For the band-to-band excitation, the third harmonics of the output of the *Q*-switched Nd^{3+} :YAG laser was used as a pump source. For site-selective excitation, the dye laser with Exalite 384 dye pumped by the third harmonics of the output of the *Q*-switched Nd^{3+} :YAG laser was used as a pump source. The spectral linewidth of the dye laser was 0.014 meV. The pulse width and repetition of the lasers were 5 ns and 30 Hz, respectively. The halogen lamp was used as a probe source. Transmittance spectra of the samples were measured by using a diode-array-type optical multichannel analyzer in conjunction with a 25-cm monochromator or a charge-coupled-device in conjunction with a 93-cm monochromator. Absorption-change spectra are defined as the difference of the absorption spectra taken before and after the sample is exposed to the laser light.

Figure 1(a) shows absorption spectra of CuCl nanocrystals embedded in a NaCl crystal at 2 K. The dash-dotted line in Fig. 1(a) represents the spectrum before the dye laser irradiation. The mean radius of the nanocrystals is 3.5 nm, estimated from SAXS experiments. The Z_3 -exciton absorption band is inhomogeneously broadened, and shows the blueshift from its position in bulk CuCl. The mean radius estimated from the blueshift (15 meV) on the exciton quan-

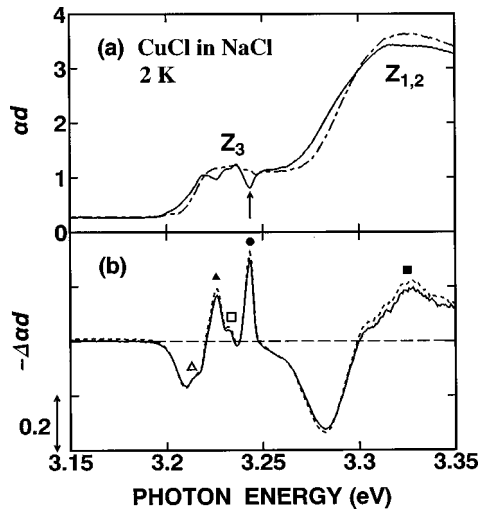


FIG. 1. Persistent spectral holes of CuCl nanocrystals embedded in a NaCl crystal at 2 K. (a) Absorption spectra before (dash-dotted line) and after (solid line) the laser exposure; (b) absorption-spectral change measured at 2 min (dotted line) and 20 min (solid line) after the burning laser is stopped. The main hole (●) and satellite holes (▲, △, ■, and □) are clearly observed. The mean radius of the nanocrystals is 3.5 nm. The burning photon energy, the energy density, the pulse duration, the pulse repetition, and the excitation period are 3.245 eV, $33 \mu\text{J}/\text{cm}^2$, 5 ns, 30 Hz, and 3 min, respectively.

tum confinement model⁹ is 3.3 nm, almost consistent with the SAXS results. The absorption spectrum is changed after the dye laser exposure, as indicated by a solid line in Fig. 1(a). Figure 1(b) shows the absorption-spectral change of the sample. The hole spectra were recorded at 2 min (dotted line) and at 20 min (solid line) after the laser exposure was stopped. The spectral holes are preserved for more than 20 min, much longer than the exciton lifetime.³ Further, we confirmed the persistency of the holes for several hours. The hole spectrum is more complicated than that of CuCl nanocrystals embedded in glass.³ The main spectral holes are superposed on the large wavy structures coming from the redshiftlike spectral change of the absorption band. Satellite holes are also clearly observed: The solid circle (●) in Fig. 1(b) indicates the main hole; the open triangle (△) the LO-phonon sideband; the solid triangle (▲) the TO-phonon sideband; the open square (□) the sideband of the TA-phonon at the Brillouin-zone edge; the solid square (■) the sideband related to the $Z_{1,2}$ excitons.

We found that the hole depth and the wavy structure coming from the redshiftlike spectral changes grow nearly in proportion to the logarithm of the laser exposure time, similar to CuBr and CuI nanocrystals embedded in glass^{3,10} and dye-doped organic glass.¹¹ The logarithmic hole growth is due to a broad distribution of the hole-burning rate. The PSHB phenomena can be explained by tunneling from one site to another through the potential barrier with distributed barrier height and width, which is called a double-well potential model or TLS model.¹²

The hole structures are erasable by the temperature rise. Figure 2 shows (a) absorption spectrum, (b) hole spectra after various temperature cycles, and (c) the hole area plotted as a function of the cycling temperature. This experimental sequence is as follows: At first, the spectral holes are burned

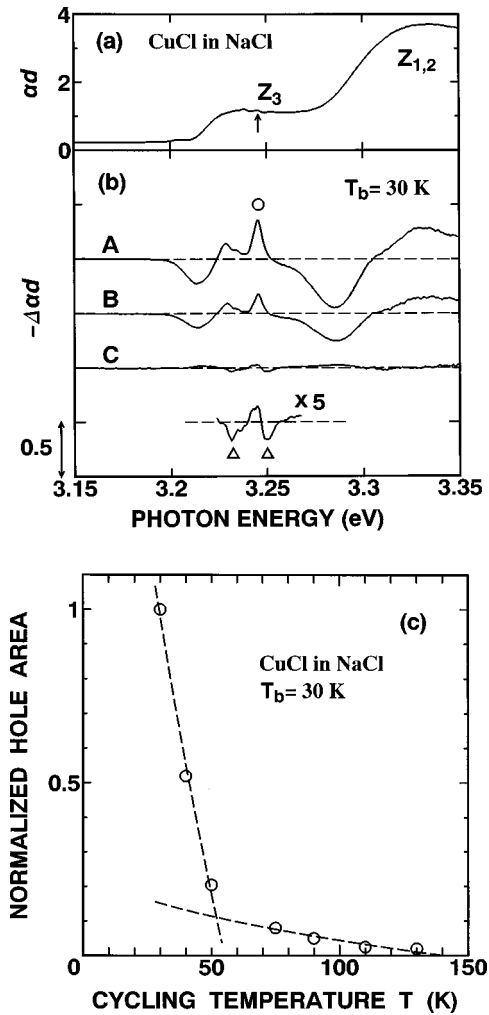


FIG. 2. Spectral holes of thermally annealed CuCl nanocrystals embedded in a NaCl crystal after the intense laser exposure as a function of the cycling temperatures. (a) Absorption spectrum; (b) absorption-spectral change recorded after the various temperature cycles: (A) 30, (B) 45, and (C) 75 K. Open circle (○) and triangles (△) represent the main hole and antiholes, respectively. (c) Normalized hole area of CuCl nanocrystals as a function of the cycling temperature T . After hole-burning at T_b and cycling through the elevated temperature T , the hole is measured at T_b again. The dashed lines represent the calculated results on the model described in Ref. 13 and are fit by the following expressions; $0.15(1 - 0.016\sqrt{T})/(1 - 0.016\sqrt{30})$ [$T > 50$ K] and $0.15(1 - 0.016\sqrt{T})/(1 - 0.016\sqrt{30}) + 0.85(1 - 0.084\sqrt{T})/(1 - 0.084\sqrt{30})$ [$T < 50$ K]. The mean radius of the nanocrystals is 3.5 nm. The hole-burning temperature T_b is 30 K. The temperature-cycling measurements were done after the 1-min laser exposure at the pump photon energies of 3.245 eV with the energy density of $40 \mu\text{J}/\text{cm}^2$.

at certain temperature T_b , and the hole spectrum is measured; after cycling through the elevated temperature (cycling temperature) T , the hole spectrum is measured again at T_b . The experimental cycling-temperature dependence of hole filling is well expressed by the thermal activation model across distributed barrier height.¹³ The rate of this model is expressed by $\nu = \nu_0 \exp(-V/kT)$, where ν_0 is the frequency factor which is the order of 10^{11} s^{-1} and V the potential barrier height. During the holding time t at the temperature T , the hole is filled if the condition $\nu t > 1$ holds. Therefore,

the hole is filled, if $V < kT \ln(\nu_0 t)$. Moreover, we assume that the distribution of the potential barrier height $P(V)$ is expressed by $P(V) \propto 1/\sqrt{V}$ with a maximum barrier height $V_{0\text{max}}$.¹³ The annealing temperature-dependent hole area have been fitted by the functional form of $[1 - \sqrt{kT \ln(\nu_0 t)/V_{0\text{max}}}] / [1 - \sqrt{kT_b \ln(\nu_0 t)/V_{0\text{max}}}]$ for $kT \ln(\nu_0 t) < V_{0\text{max}}$ in the case of dye molecules in organic glass.¹³ Here, $\ln(\nu_0 t)$ is the logarithm of the product of the attempt frequency (ν_0) and the holding time (t), and is given by 32–35. We tried to fit the expression to the experimental results and estimated the maximum barrier height $V_{0\text{max}}$ between the TLS. Two components are necessary to account for the data. The maximum barrier height is 140–160 meV for $T < 50$ K and 400–420 meV for $T > 50$ K. The absorption-change spectra abruptly varied after the temperature cycles above 50 K, as displayed in Fig. 2(b): After the temperature cycles above 50 K, the large wavy structures coming from redshiftlike spectral changes almost disappear, and antiholes, induced absorption adjacent to the spectral hole $[\Delta$ in Fig. 2(b)], appear. Antiholes are important signs that the PSHB phenomena are photophysical,¹² e.g., local-environmental changes around the nanocrystals. After the temperature cycles above 150 K, the spectral hole almost disappears. These observations prove the coexistence of two kinds of TLS's in the sample. The cycling temperature dependence is almost independent of the energy positions of the burned holes.

We found correlations between the absorption spectral changes showing PSHB phenomena and PL spectral-changes of excitons and Cu^+ dimers. Figures 3(a), 3(b), and 3(c) show absorption, absorption-change spectra, and PL spectra after the laser irradiation with the 3.492-eV excitation energy, respectively, at 2 K. The excitation source was the third harmonics of the output of the Q -switched Nd^{3+} :YAG laser. This experimental sequence is as follows: At first, absorption spectrum before the laser exposure is measured. Next, the band-to-band excitation of the sample is started and, during the first 10 s of exposure, PL spectrum is measured. After the sample is exposed for a certain time (300 or 3000 s, in this experiment), the laser exposure is stopped, and then the absorption spectrum is measured. After that, the PL spectrum is measured again. The PL-data accumulated time is 10 s.

In this case, the absorption-change spectra show the wavy structures coming from redshiftlike spectral change and the bleaching of the Z_3 -exciton absorption band but do not show spectral holes. This is because the band-to-band transition occurs under the pump photon energy. Laser irradiation induces not only absorption-spectral changes but also PL-spectral changes.¹⁴ At first, PL peak energy was at the Z_3 -exciton absorption peak energy (●). With an increase of the laser irradiation time, another PL peak (×) grew and the absorption spectrum was modified. Moreover, we found that the peak of the PL spectra (×) in the well-irradiated sample is at almost the same energy position as the lowest-energy peak of the absorption-change (○). Using the nanocrystal samples with various mean radius, we determined the relations between the Z_3 -exciton absorption peak energy (●), the lowest-energy peak of the absorption-change (○), and the peak energy of the PL spectra (×). The results are plotted in Fig. 3(d). With the decrease of the Z_3 -exciton absorption

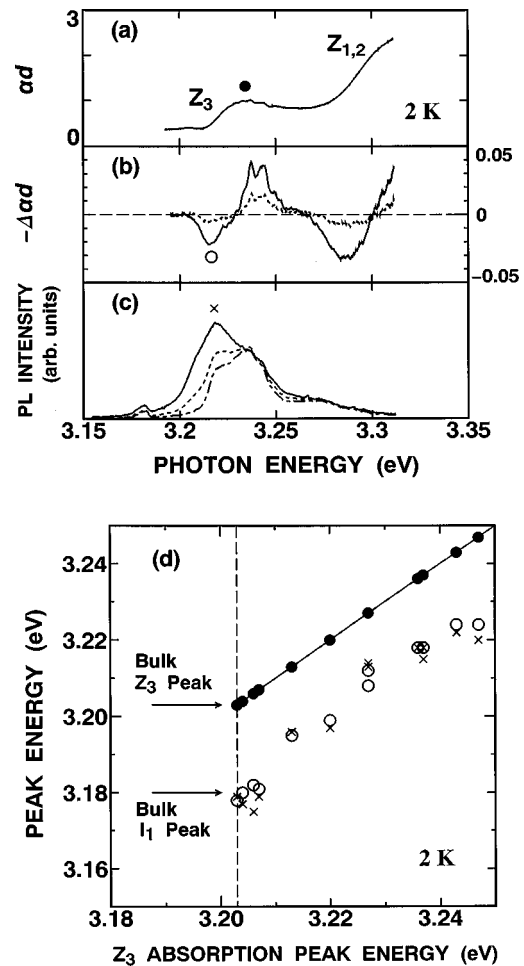


FIG. 3. Laser-exposure time dependence of absorption- and photoluminescence (PL) spectra of CuCl nanocrystals embedded in a NaCl crystal under the 3.492-eV laser excitation with the 30-Hz pulse repetition and the $0.85\text{-}\mu\text{J}/\text{cm}^2$ energy density at 2 K. (a) Absorption spectrum; (b) absorption-change spectra measured at 300 s (dotted line) and 3000 s (solid line) after the laser exposure; (c) PL spectra measured at 0 s (dash-dotted line), 300 s (dotted line), and 3000 s (solid line) after the laser exposure is started. The PL-data accumulated time is 10 s. (d) Peak energies of Z_3 -exciton absorption spectra (●) vs those of well-exposed absorption-change spectra (○) and of well-exposed PL spectra (×). Horizontal axis also represents the peak energies of Z_3 -exciton absorption spectra.

peak energy (●), i.e., the increase of the mean radius of the nanocrystals, the lowest-energy peak of the absorption-change (○), and the peak energy of the PL spectra (×) approach to the energy position of the I_1 center of bulk CuCl crystal: I_1 center is attributed to excitons bound to neutral acceptors made of Cu^+ vacancies in CuCl .¹⁵ They probably contain the charged exciton components as shown in Ref. 14. This result suggests that the observed peaks (○ and ×) are correlated with I_1 centers, namely, Cu^+ -ion vacancies in CuCl nanocrystals and resultant charge instability of the nanocrystals.

Moreover, we found that the PL spectra as well as the absorption-change spectra change with an increase of cycling temperatures: After the temperature cycles above 50 K, the absorption spectral changes, i.e., wavy structures coming from redshiftlike absorption change, almost disappear. This observation is consistent with the abrupt spectral change ob-

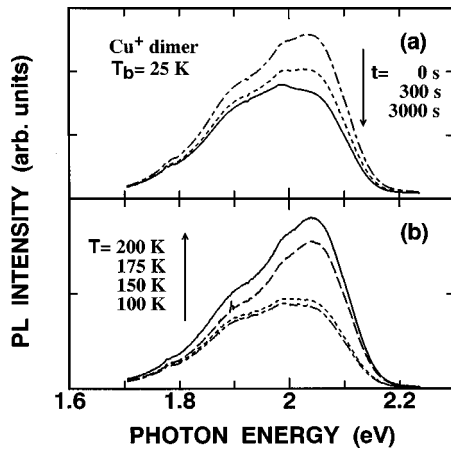


FIG. 4. Photoluminescence (PL) spectral-change of Cu^+ dimers at $T_b = 25$ K under the 3.492-eV and 30-Hz excitation. (a) PL spectra measured at 0 s (dash-dotted line), 300 s (dotted line), and 3000 s (solid line) after the laser exposure with the $8.5\text{-}\mu\text{J}/\text{cm}^2$ energy density is started. The PL-data accumulated time is 10 s. (b) PL spectra after the various temperature cycles: 100 K (dash-dotted line), 150 K (dotted line), 175 K (dashed line), and 200 K (solid line) under the laser irradiation with the $420\text{-nJ}/\text{cm}^2$ energy density. The temperature-cycling measurements were done after the 1-min laser exposure with the $850\text{-}\mu\text{J}/\text{cm}^2$ energy density.

served at 50 K, as shown in Fig 2(b). Simultaneously, the PL spectra returned to the spectra observed before the intense laser irradiation. This can be explained by considering that I_1 centers, namely, Cu^+ -ion vacancies, and resultant charge instability were reduced by thermal activation.

PL spectral changes triggered by Cu^+ -ion displacements are observed not only in CuCl nanocrystals but also in a NaCl crystal. Figure 4 shows PL spectra at around 2.1 eV in CuCl nanocrystals embedded in a NaCl crystal. The sample was the same as used in Figs. 1–3. The PL band in Fig. 4 is ascribed to Cu^+ dimers in a NaCl crystal since the PL lifetime (50 μs), the bandwidth (0.2 eV), and the peak position (2.1 eV) are consistent with those of Cu^+ dimers at low temperatures reported in Refs. 16–18. It is reasonable to expect that CuCl nanocrystals are surrounded by Cu^+ dimers since the nanocrystals are formed by aggregation of Cu^+ ions.^{9,16} At 25 K, the PL ascribed to Cu^+ dimers decreases its intensity with the increase of the laser irradiation time, as shown in Fig. 4(a). Moreover, after the PL spectra of the dimers are sufficiently changed by the intense laser irradiation, the PL intensity increases with the increase of the cycling temperature and quickly recovers when the cycling temperature exceeds 150 K, as shown in Fig. 4(b). These observations can be explained by photodissolution of Cu^+ dimers and thermal aggregation of Cu^+ monomers. The phenomena are considered to occur via the ion-exchange between Na^+ and Cu^+ ions, similar to Cu^+ ions in Cu^{2+} -doped $\text{Na}^+ \text{-}\beta''\text{-alumina}$.¹⁷

The cycling-temperature dependence of recovery of the PL and absorption spectra are correlated with the return movement of Cu^+ ions in CuCl nanocrystals and in a NaCl crystal to the previous sites after the temperature cycles above 50 and 150 K, respectively. The cycling-temperature dependence of the PL spectral change due to the movement of Cu^+ ions coincides with that of the PSHB phenomena.

Here, it should be noted that the potential barrier heights obtained from the temperature-cycling experiments in the PSHB phenomena are almost consistent with those for Cu^+ -ion displacements in CuCl and NaCl crystals obtained from *ab initio* calculations: from the temperature-cycling experiments, potential barrier heights were estimated to be 140–160 and 400–420 meV; from *ab initio* calculations, potential barrier heights are estimated to be 120 (Ref. 4) and 180 meV (Ref. 5) for Cu^+ -ion displacements between on- and off-center sites in bulk CuCl, and to 160–870 meV for a formation of a Cu^+ site in NaCl crystals via $\text{Na}^+ \text{-Cu}^+$ ion exchange.¹⁹ Thus, barrier heights of 140–160 meV obtained from the temperature-cycling experiments corresponds to those for Cu^+ -ion displacement in CuCl nanocrystals, and the barrier heights of 400–420 meV to those for Cu^+ -ion displacement in NaCl crystals.

Observed facts suggest the strong correlation between the Cu^+ displacements and the PSHB phenomena. Although we cannot explain the persistent spectral-change quantitatively, we speculate a possible PSHB mechanism as follows. Laser irradiation on the samples induces two types of Cu^+ displacements: one occurs in CuCl nanocrystals and the other in a NaCl crystal. These processes result in photocreation of I_1 centers in CuCl nanocrystals and photodissolution of Cu^+ dimers in a NaCl crystal. The photocreation of I_1 centers and resultant charge instability forms new absorption band at the lower-energy side of the Z_3 -exciton absorption band, and then reduces the Z_3 -exciton absorption band. At the same time, the Cu^+ -ion displacement can affect the $Z_{1,2}$ excitons. The Cu^+ -ion displacement forms a new absorption band at the lower-energy side of the $Z_{1,2}$ -exciton absorption band, and then reduces the $Z_{1,2}$ -exciton absorption band, like the I_1 center. This is a possible origin of the large wavy structure coming from the redshiftlike absorption change and some of spectral hole. On the other hand, the photodissolution of Cu^+ dimers to Cu^+ monomers around nanocrystals induces local-environmental changes, e.g., the change of the number of carriers trapped in matrix defects, or/and local-distortional change caused by the $\text{Cu}^+ \text{-Na}^+$ exchange around the nanocrystals. The environmental changes probably perturb the excitons in nanocrystals. This is a possible origin of antiholes and some of spectral hole. Thus, the absorption changes due to the Cu^+ displacements inside and outside of the nanocrystals simultaneously occur under the laser exposure. When the cycling temperature is below 50 K, most of Cu^+ ions in CuCl nanocrystals and a NaCl crystal will not return to the sites before the intense laser irradiation. When the cycling temperature is above 50 K, most of Cu^+ ions in CuCl nanocrystals return to the previous sites, and then I_1 centers and charged exciton bands disappear: wavy structures and some of the spectral hole disappears. On the other hand, Cu^+ ions in a NaCl crystal do not return because the potential barrier is higher. As a result, only the spectral change attributed to the Cu^+ -displacements in a NaCl crystal remains, and then the abrupt spectral changes, i.e., antiholes are observed [spectrum C in Fig. 2(b)]. The spectral change vanishes after the temperature cycles above 150 K.

In conclusion, we have reported on the PSHB phenomena of CuCl nanocrystals embedded in a NaCl crystal. The experimental results show that the PSHB phenomena can be explained by two types of TLS's. The PSHB and PL

spectral-change phenomena can be triggered by photoinduced Cu⁺-ion displacements in CuCl nanocrystals and a NaCl crystal.

Small-angle x-ray scattering experiments were done by the approval of the Photon Factory (PF) Advisory Committee (Proposals 90-222 and 92-117). We wish to acknowledge

Professor Y. Amemiya at PF for his gentle guidance to the experiments. This work was done under the TARA (Tsukuba Advanced Research Alliance) project at the University of Tsukuba. S.O. is grateful to the JSPS Research Associate Program ("Research for the Future" Program from the Japan Society for the Promotion of Science, No. JSPS-RFTF96R12501).

*Present address: Faculty of Engineering, Tokyo Engineering University, 1404-1 Katakura, Hachiohji, Tokyo 192, Japan. Also at Department of Electrical and Electronic Engineering, Faculty of Engineering, Tottori University, Koyama, Tottori 680, Japan.

¹A. I. Ekimov, A. L. Efros, and A. A. Onushchenko, *Solid State Commun.* **56**, 921 (1985).

²L. Brus, *IEEE J. Quantum Electron.* **QE-22**, 1909 (1986).

³See, for example, Y. Masumoto, *J. Lumin.* **70**, 386 (1996).

⁴S.-H. Wei, S. B. Zhang, and A. Zunger, *Phys. Rev. Lett.* **70**, 1639 (1993).

⁵C. H. Park and D. J. Chadi, *Phys. Rev. Lett.* **76**, 2314 (1996).

⁶D. V. Lang and R. A. Logan, *Phys. Rev. Lett.* **39**, 635 (1977).

⁷A. Göbel, T. Ruf, M. Cardona, C. T. Lin, and J. C. Merle, *Phys. Rev. Lett.* **77**, 2591 (1996); C. H. Park and D. J. Chadi, *ibid.* **77**, 2592 (1996).

⁸Y. Masumoto, M. Yamazaki, and H. Sugawara, *Appl. Phys. Lett.* **53**, 1527 (1988).

⁹T. Itoh, Y. Iwabuchi, and M. Kataoka, *Phys. Status Solidi B* **145**, 567 (1988).

¹⁰Y. Masumoto, K. Kawabata, and T. Kawazoe, *Phys. Rev. B* **52**, 7834 (1995).

¹¹R. Jankowiak, R. Richert, and H. Bässler, *J. Phys. Chem.* **89**, 4569 (1985).

¹²*Persistent Spectral Hole-Burning: Science and Applications*, edited by W. E. Moerner (Springer-Verlag, Berlin, 1988).

¹³W. Köhler, J. Meiler, and J. Friedrich, *Phys. Rev. B* **35**, 4031 (1987).

¹⁴T. Kawazoe and Y. Masumoto, *Phys. Rev. Lett.* **77**, 4942 (1996).

¹⁵M. Certier, C. Wecker, and S. Nikitine, *J. Phys. Chem. Solids* **30**, 2135 (1969).

¹⁶S. A. Payne, L. L. Chase, and L. A. Boatner, *J. Lumin.* **35**, 171 (1986).

¹⁷J. D. Barrie, B. Dunn, G. Hollingsworth, and J. I. Zink, *J. Phys. Chem.* **93**, 3958 (1989).

¹⁸H. Kishishita, *Phys. Status Solidi B* **55**, 399 (1973).

¹⁹V. Luaña and M. Flórez, *J. Chem. Phys.* **97**, 6544 (1992); M. Flórez, M. A. Blanco, V. Luaña, and L. Pueyo, *Phys. Rev. B* **49**, 69 (1994).